DOI: 10.1002/chem.200901300

Influence of Gold Nanoparticles of Varying Size in Improving the Lipase Activity within Cationic Reverse Micelles

Subhabrata Maiti, Dibyendu Das, Anshupriya Shome, and Prasanta Kumar Das*[a]

Abstract: Herein, we report the effect of gold nanoparticles (GNPs) in enhancing lipase activity in reverse micelles of cetyltrimethylammonium bromide (CTAB)/water/isooctane/*n*-hexanol. The size and concentration of the nanoparticles were varied and their specific roles were assessed in detail. An overall enhancement of activity was observed in the GNP-doped CTAB reverse micelles. The improvement in activity becomes more prominent with increasing concentration and size of the GNPs (0–52 μM and ca. 3–30 nm, respectively). The observed highest lipase activity ($k_2 = 1070 \pm 12\ cm^3 g^{-1} s^{-1}$) in GNP-doped CTAB reverse micelles ([GNP]: 52 μM, ca. 20 nm) is 2.5-fold higher than in CTAB reverse micelles without GNPs. Improvement in the lipase activity is only specific to the GNP-doped reverse micellar media, whereas GNP deactivates and structurally deforms the enzyme in aqueous media. The reason for this activation is probably due to the formation of larger-sized reverse micelles in which the GNP acts as a polar core and the surfactants aggregate around the nanoparticle ('GNP pool') instead of only water. Lipase at the augmented interface of the GNP-doped reverse micelle showed improved activity because of enhancement in both the substrate and enzyme concentrations and increased flexibility in the lipase conformation. The extent of the activation is greater in the case of the larger-sized GNPs. A correlation has been established between the activity of lipase and its secondary structure by using circular dichroism and FTIR spectroscopic analysis. The generalized influence of GNP is verified in the reverse micelles of another surfactant, namely, cetyltripropylammonium bromide (CTPAB). TEM, dynamic light scattering (DLS), and UV/Vis spectroscopic analysis were utilized to characterize the GNPs and the organized aggregates. For the first time, CTAB-based reverse micelles have been found to be an excellent host for lipase simply by doping with appropriately sized GNPs.

Keywords: enzyme activity · gold · lipase · nanoparticles · reverse micelles · surfactants

Introduction

Gold nanoparticles (GNPs) are consistently achieving an exponential importance in diversified fields, including materials science, electronics, nanobiotechnology, and so forth, because of their unique optical,[1] electronic,[2] and molecular-recognition properties.[3–6] Interestingly, applications of these stable metal nanoparticles in biology, the life sciences, and biomedicines are rapidly growing, such as chemical sensing and imaging applications.[7] Recently, efforts have been made to investigate the role of GNPs on the modulation of enzyme activity, which can be effective for controlling cellular processes, such as signal transduction, DNA replication, and metabolism.[8,9] The high surface-to-volume ratio offered by the metal nanoparticle is one of the intrinsic characteristics that is increasing their applications exponentially in different branches of science.

To this end, the water-in-oil (w/o) microemulsion, another class of macroscopically homogenous nanometer-scale colloidal system that comprises large microscopic interfacial areas, has been extensively used as a host for enzymes and proteins.[10–15] The w/o microemulsion, also known as reverse micelles, are formed due to the self-organization of surfactants into aggregates in apolar organic solvents with 'water pools' in their polar cores. On several accounts, we have been successful in the design of novel reverse micelles by variation of the different microstructural parameters in which both interfacially solubilized enzymes, such as lipase and horseradish peroxidase,[11a,b,13d,e,14a–e] and water-pool solubilized hydrophilic enzymes, such as trypsin,[11e] have dis-

[a] S. Maiti, D. Das, A. Shome, Dr. P. K. Das
Department of Biological Chemistry
Indian Association for the Cultivation of Science
Jadavpur, Kolkata 700032 (India)
Fax: (+91) 33-24732805
E-mail: bcpkd@iacs.res.in

Supporting information for this article is available on the WWW under http://dx.doi.org/10.1002/chem.200901300.

played superior activity in these nanoreactors. In most of the cases, it has been seen that the 'space' or surface area in the vicinity of the enzyme plays the most crucial role in modulating the catalytic activity of the enzyme.[13e,14a,b,e] Enzymes localized at the enhanced surface area always exhibited improvement in activity due to the increased substrate concentration and also by attaining a flexible conformation. At this point, we were curious to investigate whether GNPs of varying dimensions with proportionate surface areas could also regulate the activity of enzymes encapsulated in these reverse micelles. Incorporation of the colloidal gold particles inside the water core of the reverse micelle is expected to alter the microstructural parameters of the system. Consequently, the enzyme might face a considerably renewed microenvironment in its vicinity. Although there have been a lot of reports on the synthesis of nanoparticles of varying size within the reverse-micellar system already,[5f] how enzyme activity can be affected in reverse micellar system in the presence of GNPs has not been reported so far.

Herein, we have investigated how the catalytic efficiency of *Chromobacterium viscosum* (CV) lipase is influenced in GNP-doped cationic reverse micelles of cetyltrimethylammonium bromide (CTAB)/isooctane/*n*-hexanol/water across a wide range of [water]/[surfactant] ratios (W_0). Lipase showed a notable enhancement in its activity when GNP was doped in CTAB reverse micelles, and the enzyme activity steadily increased with increase in the GNP concentration. Strikingly, in the CTAB reverse micelle, lipase showed an enhancement in activity with an increase in the W_0 value in the presence of GNPs for the first time. The best lipase activity ($k_2 = 1070 \pm 12\ cm^3 g^{-1} s^{-1}$) was found when the ratio of [*n*-hexanol]/[surfactant] (z) was 4.8, $W_0 = 52$, and [GNP] = 52 μM and is 2.5-fold higher than the activity of lipase in CTAB reverse micelles without GNPs under identical experimental conditions. The enzyme activity improved with an increase in the size of the GNPs. The structural changes of lipase in water and self-aggregates were monitored through circular dichroism (CD) and FTIR spectroscopic analysis. The generalized influence of GNP is verified in reverse micelles of another surfactant, that is, cetyltripropylammonium bromide (CTPAB). Hence, without changing the basic structure of the surfactant, we have established for the first time that simple a CTAB reverse micelle can also be a suitable host for lipase in the presence of GNPs of an appropriate size.

Results and Discussion

In this study, our main aim is to delineate the effect of GNPs of varying size on the supramolecular structure of the cationic reverse micelle, and consequently on the catalytic activity of surface-active lipase entrapped in that microemulsion.

For this purpose, we synthesized GNPs from [$HAuCl_4$] by following a standard procedure[5b,d,e] with trisodium citrate, which acts as a reducing and stabilizing agent. The solution of GNP in water showed a surface plasmon resonance (SPR) peak at 528 nm (GNP_{528}; Figure 1a) and the size of the GNPs was found to be approximately 15–20 nm from TEM images (Figure 1b). However, the hydrodynamic diameter D_h of the same GNP_{528} was found to be 34 ± 4 nm when measured in dynamic light scattering (DLS) experiments. Such a difference in the size when measured by two different techniques is known to occur because TEM is only sensitive to the electron-rich metal particle, whereas DLS measures the total size of the GNP including the hydrated layer of the ligand/stabilizer, namely, citrate in the present study.[5g,h] The synthesized GNP_{528} were doped in reverse micelles of CTAB (50 mM)/isooctane/*n*-hexanol/water. Importantly, the size of the externally synthesized GNP_{528} did not alter after doping in the reverse micelles (see Figure S1 in the Supporting Information). In this GNP-doped reverse micelle, lipase was added followed by *p*-nitrophenyl *n*-octanoate. The overall concentrations of the lipase and substrate

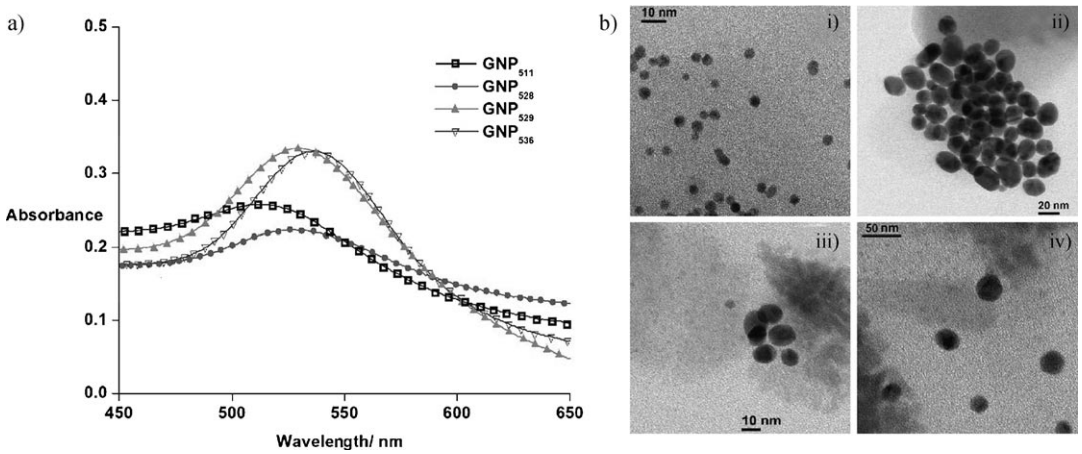

Figure 1. a) SPR peaks of GNPs of varying sizes: GNP_{511}, GNP_{528}, GNP_{529}, and GNP_{536}. b) TEM images of i) GNP_{511}, ii) GNP_{528}, iii) GNP_{529}, and iv) GNP_{536}.

were 1.02 μg mL^{-1} and 3.0 mM, respectively. Enzymatic hydrolysis was monitored by measuring the absorbance of liberated *p*-nitrophenol at the isosbestic point (see Table S1 in the Supporting Information). At the onset, we found that the CV lipase-catalyzed hydrolysis of *p*-nitrophenyl *n*-octanoate in GNP_{528}-doped cationic reverse micelles also follows second-order kinetics, as conventionally shown by lipase in other w/o microemulsions[11a,13d,15,16] (see Figure S2). Initially, lipase activity at $z=4.8$ was observed across a W_0 range of 44–52 in the CTAB reverse micelle at varying concentrations of GNP_{528} (0–44 μM; Figure 2). A minimum amount of

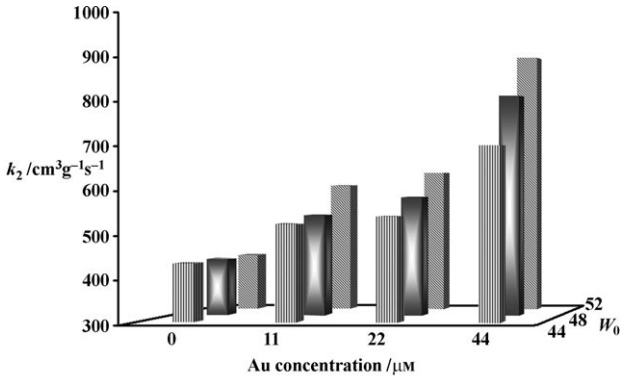

Figure 2. Variation of the second-order rate constant k_2 for the lipase-catalyzed hydrolysis of *p*-nitrophenyl *n*-octanoate in GNP-doped CTAB reverse micelles with varying W_0 values and GNP concentrations at $z=4.8$ and 25 °C. [CTAB] = 50 mM, [enzyme] = 1.02×10^{-6} g mL^{-1}, [substrate] = 3 mM. Experimental errors are within ±1–2 %.

n-hexanol was used to prepare the reverse micelles to decrease the inhibitory action[11a,14d,17] of alcohols on the catalytic activity of lipase. It was observed that lipase activity increased with increasing GNP (Au) concentration. At $z=4.8$ and $W_0=44$, the second-order rate constant k_2 of lipase increased from 433 ± 7 to 694 ± 8 cm^{3}g^{-1}s^{-1} on increasing the concentration of GNP_{528} from 0 to 44 μM (Figure 2). Interestingly, the extent of the enhancement in the lipase activity on increasing the concentration of GNP_{528} was greater for a higher W_0 value because the k_2 value increased almost 100 % from 433 ± 7 to 825 ± 9 and 926 ± 10 cm^{3}g^{-1}s^{-1} at $W_0=48$ and 52, respectively (Figure 2). Encouragingly, it was possible to increase the concentration of GNP_{528} up to 52 μM ($W_0=52$), at which the lipase activity enhanced further to a maximum of 1070 ± 12 cm^{3}g^{-1}s^{-1}, that is, 2.5-fold higher than the activity of lipase in CTAB reverse micelles (433 ± 7 cm^{3}g^{-1}s^{-1}) without GNPs.

The influence of GNP_{528} on the activity of lipase was also tested in different compositions of w/o microemulsions with a higher *n*-hexanol content. The reason for using a higher amount of cosurfactant was to find out whether the activating effect of GNPs has dominance over the inhibitory action of *n*-hexanol. An almost 1.7-fold enhancement in lipase activity was observed in the range $W_0=36$–44 with increasing concentrations of GNP_{528} (0–36 μM) at $z=6.4$ and 8.0, at which the k_2 value increased from 365 ± 7 to 615 ± 6 cm^{3}g^{-1}s^{-1} and 350 ± 6 to 600 ± 8 cm^{3}g^{-1}s^{-1}, respectively (Figure 3a,b). The absolute lipase activity and activation effect were further decreased to 1.4–1.5-fold when the *n*-

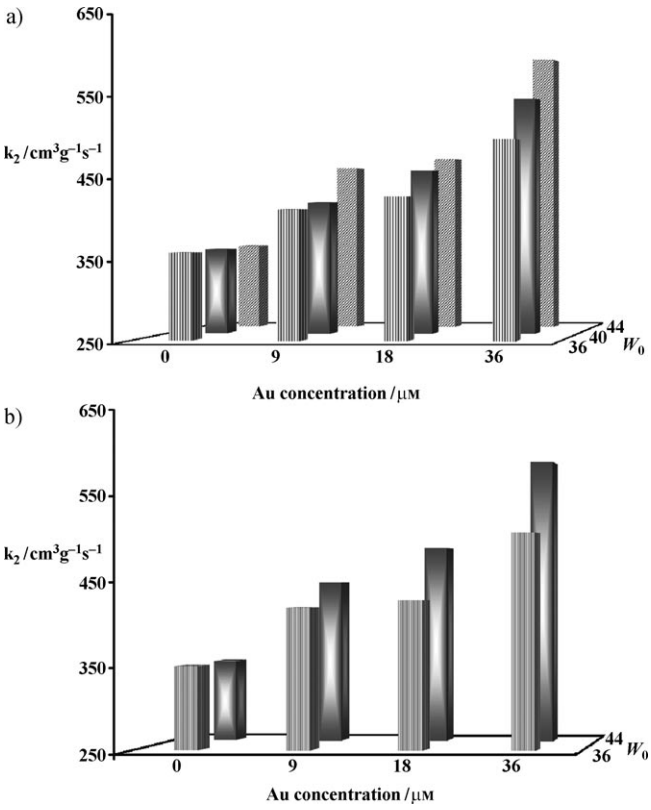

Figure 3. Variation of the secondorder rate constant k_2 for the lipase-catalyzed hydrolysis of *p*-nitrophenyl *n*-octanoate in GNP-doped CTAB reverse micelles with varying W_0 values and GNP concentrations at $z=6.4$ (a) and 8.0 (b) and 25 °C. [CTAB] = 50 mM, [enzyme] = 1.02×10^{-6} g mL^{-1}, [substrate] = 3 mM. Experimental errors are within ±1–2 %.

hexanol content was increased to $z=11.2$ and 16.0 (see Table S2). At $z=11.2$ and 16.0 and $W_0=24$, the lipase activity modestly increased from 284 ± 5 to 404 ± 6 cm^{3}g^{-1}s^{-1} and 210 ± 5 to 315 ± 8 cm^{3}g^{-1}s^{-1}, respectively, on increasing the concentration of GNP_{528} (0–22 μM). Although the activation effect in GNP_{528}-doped reverse micelles decreased with increasing *z* values, the trend is similar as the lipase activity increased on increasing the concentration of the GNPs (Figure 2, Figure 3, and Table S2 in the Supporting Information). Hence, GNP_{528} with an average size of 15–20 nm have a generalized activating effect on the catalytic efficiency of the surface-active enzyme lipase in CTAB reverse micelles.

Another interesting trend seen in the present study is the variation of lipase activity with the W_0 value in the presence of GNPs. Till date, lipase activity in CTAB reverse micelles remained unaltered with changes in the W_0 value. This behavior is also consistent in the present study because lipase activity did not change with the W_0 value in the absence of GNPs. At $z=4.8$, 6.4, and 8.0, k_2 = 433 ± 7, 365 ± 7, and 350 ± 6 cm^{3}g^{-1}s^{-1}, respectively, for $W_0=36$–52 in CTAB systems without GNPs. In contrast, at a given *z* value and a

fixed concentration of GNP_{528}, the lipase activity was enhanced with an increase in W_0 value (Figures 2 and 3). For example, at $z=4.8$ and $[GNP_{528}]=44\ \mu M$, there was an increase from $k_2=703\pm10$ to $926\pm10\ cm^3\,g^{-1}\,s^{-1}$ with an increase from $W_0=44$ to 52 (see Figure S3 in the Supporting Information). Similarly at $z=6.4$ and $[GNP_{528}]=36\ \mu M$, there was an increase from $k_2=500\pm8$ to $615\pm6\ cm^3\,g^{-1}\,s^{-1}$ with an increase from $W_0=36$ to 44, whereas there was an increase from $k_2=424\pm6$ to $504\pm7\ cm^3\,g^{-1}\,s^{-1}$ at $z=8.0$ and $[GNP_{528}]=26\ \mu M$ when there was an increase from $W_0=28$ to 44 (see Figure S3 in the Supporting Information). Thus, lipase activity increased in CTAB reverse micelles with an increase in the W_0 value in the presence of GNPs for the first time.

To understand the rationale for the observed enhancement in lipase activity with increasing concentrations of GNP_{528} and the W_0 value, it is necessary first of all to know how the same nanoparticle influences the structure–activity relationship of lipase in aqueous solution. To this end, lipase activity ($0.02\ \mu g\,mL^{-1}$) was investigated in aqueous solution (water + 4% EtOH) with *p*-nitrophenyl *n*-hexanoate (0.06 mM) as a substrate in the presence of varying concentrations of GNP_{528} (Table 1).[16] The lipase activity steadily

Table 1. Secondary structure of lipase and the GNP/lipase mixture in water determined by FTIR spectra and second-order rate constant k_2 for the lipase-catalyzed hydrolysis of *p*-nitrophenyl *n*-hexanoate in water in the presence of varying concentrations of GNPs at 25 °C.

Enzyme	α Helix content [%]	β Sheet [%]	GNP (Au) concentration [μM]	k_2[a] [$cm^3\,g^{-1}\,s^{-1}$]
lipase	32.6	29.7	0	3.0×10^5
GNP/lipase	18.3	63.3	5	1.8×10^5
			20	1.2×10^5
			40	1.0×10^5
			100	0.5×10^5

[a] $[enzyme]=0.02\times10^{-6}\ g\,mL^{-1}$, [substrate] = 0.06 mM.

decreased sixfold as the concentration of the GNPs (i.e., Au) was increased up to 100 μM in water. The loss in the enzyme activity was correlated with the secondary structure of the lipase ($10\ \mu g\,mL^{-1}$ to obtain a measurable signal) in water by using CD spectroscopic analysis. The secondary structure of the proteins are shown in CD spectra in the far-UV region and the mean residue ellipticity (MRE) at 222 nm denotes the α-helix content of the protein.[18] The spectra revealed that in the presence of GNP_{528}, lipase loses its α-helical content and the extent of the structural deformation increases with an increase in the concentration of GNP_{528} from 20 to 200 μM (Figure 4a). To have a quantitative idea about the secondary structure of lipase in the presence of GNP_{528}, FTIR spectroscopy was used to investigate the amide I region (1600–1700 cm^{-1}), which corresponds to the C=O stretching frequency of the peptide backbone.[14e,19] The amide I region in the FTIR spectra has been successfully used in several earlier reports to quantify the secondary structural units of proteins in aqueous solutions, aqueous/organic mixtures, and immobilized states.[14e,19] To obtain a

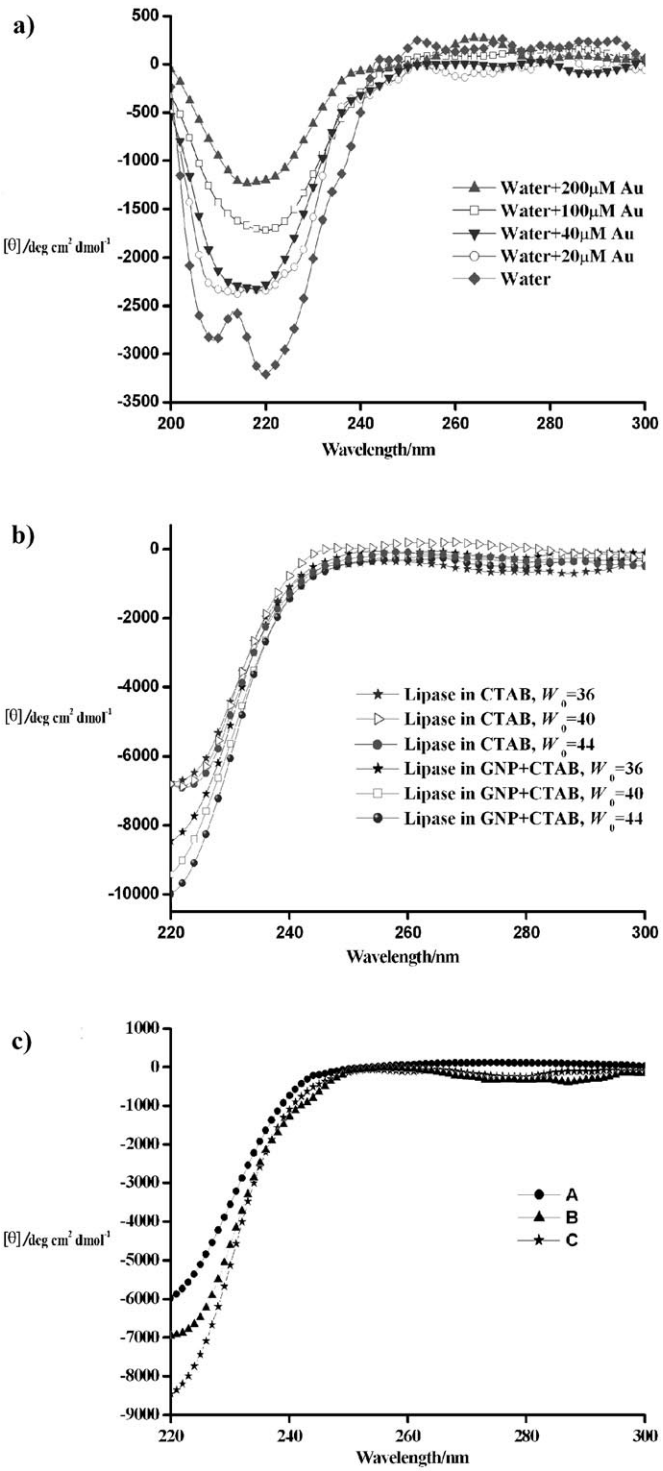

Figure 4. a) CD spectra of CV lipase in water with varying concentrations of GNPs. b) CD spectra of lipase in 50 mM CTAB reverse micelles in the absence of GNPs and in GNP-doped reverse micelles with varying W_0 values. c) CD spectra of CV lipase in CTAB reverse micelles at $W_0=40$ and $z=6.4$ with the GNP/lipase premixed solution (A), without GNPs (B), and with GNP_{528}-doped reverse micelles (C).

measurable intensity in the amide region, a high amount of lipase (170 μg) and a proportionate concentration of GNP_{528} was used for the FTIR spectroscopic study. Although the

high amount of lipase used in both the CD and FTIR spectroscopic studies may affect the GNP/lipase interaction differently relative to the activity measurements, an admissible reflection in the change of the enzyme structure is expected. In the presence of GNPs, the α-helix content of native lipase decreased from 32.6 to 18.3%, whereas the β-sheet content increased from 29.7 to 63.3% (Table 1). The association of several amino acid residues of the protein, such as lysine, aromatic amino acids, with the surface of the GNP possibly altered the secondary structure of the enzyme.[8a,20] Thus, both the CD and FTIR spectroscopic studies concurrently showed that in the presence of GNP lipase lost the α-helical content, which decreased its catalytic efficiency in water.

The obvious question that arises at this point is how the activity of lipase was selectively improved in the GNP-doped reverse micelles despite deactivation in the presence of GNPs in water. It is well known that the water-pool diameter of a CTAB reverse micelle varies from approximately 5 to 15 nm depending on the W_0 value and other microstructural parameters,[21,22] whereas the size of the citrate-reduced and capped GNP_{528} nanoparticle is approximately 20 nm (Figure 1). Thus, simple solubilization of these large GNPs within the water pool of reverse micelles is not feasible because of their comparable sizes. At this point, we were intrigued to investigate what are the dimensions of the assemblies present when GNPs are doped in the reverse micellar media. For this purpose, we carried out DLS experiments on the CTAB reverse micelles in the absence and presence of GNP_{528} and also on a solution of GNPs ($D_h = 34 \pm 4$ nm), which were doped in the reverse micelles. The D_h values of the reverse micelles without GNPs were 5.2 ± 0.5 and 11.8 ± 1 nm at $z = 11.2$ and 16.0 and $W_0 = 24$ (see Table S3 in the Supporting Information). Interestingly, in the case of the reverse micelles in which the GNPs were doped, aggregates of two different sizes were present (see Table S3 in the Supporting Information). The aggregates with smaller D_h values are similar to the size obtained in the case of the reverse micelles in the absence of GNPs. However, the size of the larger assemblies (58 ± 6 nm at $z = 11.2$ and 45 ± 3 nm at $z = 16.0$; see Table S3 in the Supporting Information) was grossly comparable to the combined D_h values of GNP_{528} (see Table S3 in the Supporting Information) and the reverse micelles in which GNPs were not present. Thus, this DLS study indicates the possible localization of the water-soluble gold colloids in the polar core of the reverse micelles.

It is necessary to understand what type of interface was formed in the GNP-doped CTAB reverse micelles. There could be two possibilities: CTAB/gold and CTAB/water interfaces. To investigate the nature of the interface present in the current system, we designed an experiment that involved the formation of GNP-doped CTAB reverse micelles in the absence of the capping agent trisodium citrate. Here, the cationic CTAB alone would be present to act as the stabilizer for the GNPs in which the GNPs are either doped in naked form or synthesized in situ. In this context, it is well known that CTAB facilitates the aggregation and assembly of GNPs.[3,5j] The TEM images of these GNPs in this particular reverse micellar system (in the absence of citrate ions) show both the aggregation and formation of irregularly shaped gold particles (see Figure S4 in the Supporting Information). These images prove that aggregation occurs when the GNPs are in contact with cationic CTAB due to the formation of a gold/CTAB interface. However, in the case of reverse micelles containing citrate-capped GNPs, we observed only spherical nonaggregated GNPs in aqueous media and after doping in the reverse micelles (Figure 1 and Figure S1 in the Supporting Information). Consequently, this outcome implies that in the presence of the citrate stabilizer, the gold/CTAB interface did not form due to the presence of the water layer (containing citrate ions) at the periphery of the nanoparticle, thereby distancing the GNP from the cationic head group of the surfactant. Therefore, it is evident from the above DLS and TEM studies that in the presence of GNP_{528} the surfactants self-organize to form larger reverse micelles around the hydrophilic GNPs as a polar core ('GNP pool') instead of only water (Scheme 1). In comparison to w/o microemulsions, the newly developed (GNP + water)-in-oil microemulsion became a better host for lipase possibly due to the reasons that will follow.

In this regard, it is important to monitor the activity of lipase in the presence of the CTAB/gold interface (irregularly shaped and without citrate ions) instead of the CTAB/water interface. No activation effect of lipase was observed in these irregularly shaped GNP-doped reverse micelles at different z values (see Table S4 in the Supporting Information). A possible reason for no activation of lipase relative to the previous case (i.e., citrate-stabilized GNP_{528}-doped reverse micelles) was probably the nonexistence of the distinct interfacial water layer. However, in the presence of citrate as the capping agent, spherical and nonaggregated gold nanoparticles were present in the reverse-micellar media (Figure 1 and Figure S1 in the Supporting Information). Therefore, in the later system the citrate stabilizers present around the surface of the GNPs in aqueous media are also retained when the GNPs are doped in the reverse micellar system or while it was synthesized in situ. Hence, there is the formation of the CTAB/water interface instead of the gold/CTAB interface in which lipase showed an improved activity. Hence, in the citrate-stabilized GNP_{528}-doped reverse micelles all water becomes a part of the interfacial region of the aggregates that accommodates the polar heads of the surfactants.

The prominent CTAB/water interfaces (in the presence of citrate ions) in the GNP_{528}-pool-based large reverse micelles can help in the smooth accommodation of lipase. It is quite obvious that the larger reverse micelle (considering its spherical shape) will surely possess a higher interfacial domain, thus offering more space for the accommodation of the enzyme and substrate. This property was reflected in the flexible conformation of lipase observed from the CD spectra (Figure 4b). As the MRE at 222 nm decreased, the α-helix content in the secondary structure of lipase increased. Second, in this augmented interfacial region of the GNP_{528}-

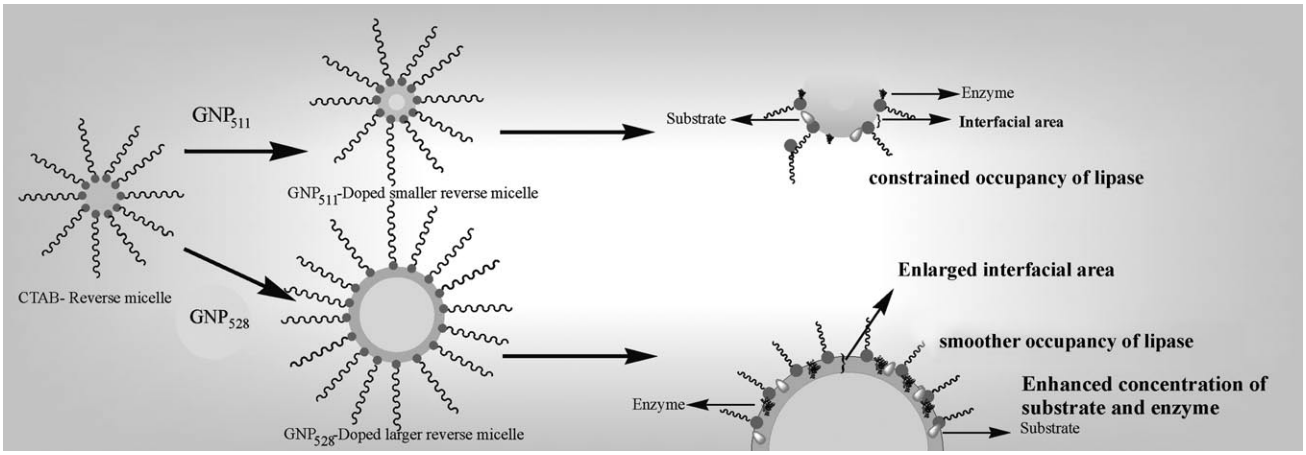

Scheme 1. Pictorial representation of lipase in GNP-doped reverse micelles.

doped reverse micelle, the population of substrate and enzyme molecules will obviously increase, thus leading to an enhancement in lipase activity. In this context, we have already established that lipase exhibits a higher catalytic ability in reverse micelles with a large head-group area of surfactant.[13e] Thus, with increasing the concentration of the GNPs, lipase activity enhanced as the number of reverse micelle with 'GNP+water' as the polar core is increased. The enhancement in lipase activity with increasing W_0 value is presumably because of the similar reason as discussed for the 'GNP-pool'-based system. The addition of more water to the system will lead to an increase in the interfacial domain around the GNPs and thereby an increase in the substrate and enzyme concentrations and flexibility in the lipase conformation. This behavior was also confirmed with the CD spectra of lipase (25 $\mu g\,mL^{-1}$) in the CTAB-reverse micelle in which MRE decreased with an increase in W_0 value, thus indicating an increase in the α-helical content of lipase while no change in the MRE was observed without GNPs (Figure 4b).

So far, we have added the lipase after the formation of the GNP-pool-based reverse micelles in which the surface-active enzyme will prefer to localize at the interfacial region. Consequently, the interaction between GNPs in the 'pool' and lipase at the 'interface' is expected to be minimum, which decreases the possibility of GNP-induced enzyme deactivation. Intriguingly, it is expected that only surface-active enzymes can avoid such deactivation. But for hydrophilic enzymes, such as trypsin, this interaction would be inevitable because both the enzyme and nanoparticle prefer to localize themselves inside the core of the water pool. Hence, we checked the activity of trypsin in water in the presence of GNP_{528} and also in GNP_{528}-doped CTAB reverse micelles (Table 2). We used *N*-α-benzyloxycarbonyl-L-lysine-*p*-nitrophenyl ester hydrochloride, a hydrophilic substrate to measure trypsin activity, in aqueous medium (pH 6.0) and reverse micelles (pH 6.0). Similar to the case of lipase, deactivation of trypsin was observed in water.[9a] The k_{cat} value of 35.2 s^{-1} decreased to $k_{cat}=29.0\,s^{-1}$ in the presence of 40 μM of GNP_{528}. Also in reverse micelles at $z=6.4$ and $W_0=40$, unlike lipase, there was an approximate 50% deactivation of trypsin from $k_{cat}=9.7$ to 4.8 s^{-1} in the presence of 40 μM GNPs. This outcome confirms the assumption of the GNP-pool model in which the nanoparticle resides in the polar core and interacts strongly with the 'water-pool-active' enzyme, thus resulting in poor activity of trypsin.

Table 2. Variation of trypsin activity k_{cat} in aqueous phosphate buffer (pH 6, 20 mM) and in CTAB reverse micelles in the presence of GNPs.

Systems		k_{cat} [s^{-1}][a]
water	without GNP	35.2
	with GNP ([Au]=40 μM)	29.0
CTAB reverse micelle (z=6.4, W_0=40)	without GNP	9.7
	with GNP ([Au]=40 μM)	4.8

[a] [Trypsin]=0.32 μM, [CTAB]=50 mM. The substrate concentrations were varied from 20 to 250 μM. In duplicate experiments, the k_{cat} values are variable within ±5–10%.

Interestingly, despite the loss of the structure and activity of both lipase and trypsin in an aqueous solution of GNPs, it is quite clear that GNP-doped CTAB reverse micelles can only act as an excellent host for the interfacially active enzyme lipase. So, we became curious to know whether the catalytic activity of structurally deprived lipase in an aqueous solution of GNP (GNP/lipase) also can be improved in CTAB reverse micelles. To evaluate this proposal, we estimated the efficiency of GNP/deactivated lipase (GNP/lipase) in the CTAB w/o microemulsion at $z=6.4$ and $W_0=40$ with varying concentrations of GNPs (Figure 5). By keeping all the other experimental conditions identical, we prepared the reverse micelles in a swirling mixture of CTAB (50 mM)/isooctane/*n*-hexanol with a premixed aqueous solution of GNP_{528}/lipase instead of adding the enzyme after the formation of GNP-doped w/o microemulsions. Interestingly, the k_2 value improved on increasing the GNP concentration and lipase showed a higher activity at any concentration of GNP (5–40 μM) than observed for native lipase (365±7 $cm^3\,g^{-1}\,s^{-1}$) in CTAB reverse micelles. At concentration of

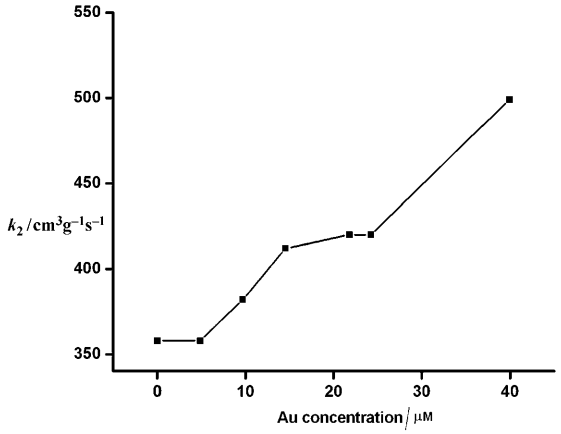

Figure 5. Variation of the second-order rate constant k_2 for the hydrolysis of *p*-nitrophenyl *n*-octanoate catalyzed by lipase added from the GNP/lipase premixed aqueous solution in CTAB reverse micelles at $z=6.4$ and $W_0=40$. The GNP concentrations were varied from 5 to 40 μM at 25 °C. [CTAB] = 50 mM, [enzyme] = 1.02×10^{-6} g mL^{-1}, [substrate] = 3 mM. Experimental errors are within ±1–2%.

40 μM for Au, the activity of lipase was enhanced up to 500 ± 8 cm^3 g^{-1} s^{-1}. Although this k_2 value is higher than the lipase activity in the CTAB reverse micelles, it is, at the same time, lower than the lipase activity in GNP_{528}-doped reverse micelles under identical experimental conditions (i.e., 615 ± 6 cm^3 g^{-1} s^{-1}; Figure 3). CD spectroscopic analysis was performed to investigate whether this deformed enzyme (premixed GNP/lipase) had experienced any improvement in its secondary structure (Figure 4c) in reverse micelles, as observed in the case for lipase in GNP-doped reverse micelles (Figure 4b). However, the premixed lipase had a lower helical content than in native lipase in reverse micelles, thus indicating that the reverse micelle is unable to revive the structure of the deformed enzyme. Consequently, it can be inferred that the structurally deprived lipase showed an improved activity in w/o microemulsions primarily due to the enhanced interfacial region in reorganized larger reverse micelles.

To establish the generality of the observed activation of lipase in citrate-capped GNP-doped w/o microemulsions, we used a cetyltripropylammonium bromide (CTPAB)-based reverse micelle as the host. The CTPAB-based reverse micelle in isooctane/*n*-hexanol is known to be an excellent host for lipase because it has a larger interfacial domain due to its high head-group area ($A_{min}=2.20\pm0.04$ nm^2).[13e] We estimated the lipase activity in GNP_{528}-doped reverse micelles of CTPAB (50 mM)/isooctane/*n*-hexanol/water at $z=4.8$ and $W_0=72$. Here also, lipase activity increased from 846 ± 9 to 1205 ± 11 cm^3 g^{-1} s^{-1} on increasing the GNP concentration from 0 to 72 μM (see Figure S5 in the Supporting Information). The extent of the activation in GNP-doped CTPAB reverse micelle was moderate relative to the GNP-doped CTAB system. This finding is probably due to lipase having the augmented space in its vicinity at the interface of the tripropylated head group of CTPAB, thus resulting in high enzyme activity (i.e., 846 ± 9 cm^3 g^{-1} s^{-1}), even in the absence of GNPs. Hence, the influence of GNP_{528} did not appear to be noteworthy in CTPAB reverse micelles because of its intrinsic high interfacial area.

Until now, we have used GNP_{528} with an average size of 15–20 nm (according to TEM; Figure 1) to investigate its effect on lipase activity in the GNP-doped reverse micelles. We have discussed above that the augmented interfacial area in the presence of GNP_{528} plays the regulatory role in improving the enzyme activity. Therefore, it is apparent that the size of this GNP also should have a crucial role in modulating the lipase efficiency. It would be intriguing to know how GNPs of varying size doped in reverse micelles would influence the activity of lipase. We synthesized three GNP of different sizes (characterized by the SPR peak in UV/Vis spectra and TEM images; Figure 1) with $NaBH_4$ as the reducing agent and citrate as the capping agent. The concentration of $NaBH_4$ was varied to obtain differently sized GNPs (see the Experimental Section for details of the synthetic procedure). The SPR peak and the corresponding average size of the GNPs are as follows: GNP_{511}: SPR peak: 511 nm, size: 3–5 nm; GNP_{529}: SPR peak: 529 nm, size: 15–20 nm; GNP_{536}: SPR peak: 536 nm, size: 25–30 nm. The lipase activity was estimated in the CTAB reverse micelles by doping the GNPs of varying sizes at a particular z and W_0 values (Table 3). Although the preceding results demonstrated that lipase showed higher activity at a higher concentration of GNPs, we took GNPs of varying size at around 11 ± 2 μM to prepare reverse micelles at a comparable concentration of GNPs of all sizes. On the whole, lipase activity is always higher in the presence of GNP irrespective of size relative to the activity in the absence of GNP. However, the extent of the improvement in lipase activity in GNP_{511}-doped reverse micelle (i.e., GNP is smaller in size) is lower than that of the comparatively larger GNP_{528}, GNP_{529}, and GNP_{536}-doped systems. Rather, the lipase activity is more or less comparable in the GNP_{529} and GNP_{536}-doped reverse micelles presumably due to the small difference in their sizes. Similarly, lipase activity in GNP_{528} and GNP_{529}-doped reverse micelles is also comparable in the identical solution compositions (see Figures 2 and 3 and Table 3). Thus, the size of the citrate-stabilized GNP is very important in regulating the enzyme activity. The interfacial domain of GNP-doped reverse micelle changes depending on the size of the GNP, which consequently alters the lipase activity.

Table 3. The second-order rate constant k_2 of the lipase-catalyzed hydrolysis of *p*-nitrophenyl *n*-octanoate in CTAB reverse micelles in the presence of GNPs of varying size.

Z	W_0	k_2 [cm^3 g^{-1} s^{-1}] without Au	Au [μM]	k_2 [cm^3 g^{-1} s^{-1}][a] GNP_{511}	GNP_{529}	GNP_{536}	GNP (in situ)
4.8	48	433 ± 7	12	484 ± 7	532 ± 8	OM[b]	480 ± 9
6.4	40	365 ± 7	10	407 ± 3	434 ± 5	441 ± 6	401 ± 7
8.0	44	350 ± 6	11	400 ± 6	449 ± 7	457 ± 8	378 ± 9
11.2	40	284 ± 5	10	354 ± 6	382 ± 5	397 ± 6	306 ± 7
16.0	32	180 ± 4	9	228 ± 7	329 ± 8	345 ± 5	203 ± 9

[a] [surfactant] = 50 mM, [enzyme] = 1.02×10^{-6} g mL^{-1}, [substrate] = 3 mM. [b] OM: opaque microemulsion; the activity could not be measured.

As of now, the GNPs used for doping in the reverse micelles were externally synthesized in aqueous solution and the size was varied by changing the concentration ratio between $[HAuCl_4]$ and $NaBH_4$. After detailed investigation into the role of externally added/doped GNPs on the activity of lipase in cationic reverse micelles, it is necessary to know how GNPs will influence the lipase when it is synthesized within the reverse-micellar water pool. The GNPs were synthesized in situ by mixing two reverse-micellar systems, one containing $[HAuCl_4]$ and trisodium citrate and another containing $NaBH_4$ (see Table 3 for the experimental solution compositions). The SPR peak of the GNPs synthesized in situ was obtained at approximately 514 nm, and the TEM image showed that the size of the GNPs varied from 5 to 8 nm (see Figure S1 in the Supporting Information). Lipase activity in the presence of GNPs synthesized in situ slightly improved relative to the activity in the absence of GNPs (Table 3). Interestingly, this small enhancement in activity is comparable to the enhancement obtained on using reverse micelles externally doped with GNP_{511} simply because of the matching sizes of the GNPs synthesized in situ and GNP_{511}. In both cases, the smaller GNPs are easily solubilized within the water pool of the reverse micelles without altering the size of the reverse micelles to a greater extent. Hence, the activation effect is not significant as the lipase experiences a more or less similar environment as in the reverse micelles without GNPs.

Conclusions

The present work describes a novel method of increasing lipase activity simply by doping GNPs of appropriate size in cationic reverse micellar systems. The enhancement in activity in reverse micelles becomes more significant because the GNPs deactivate and structurally deform lipase in aqueous solution. Lipase showed an improvement in its activity when GNPs of varying sizes were doped in the reverse micelles and the activation effect was enhanced with an increase in the size of the GNPs. We presume that the GNP acts as a polar core and the surfactants aggregate around the nanoparticle ('GNP pool') instead of only water, thus resulting in the formation of larger reverse micelles with an augmented interface, which results in a higher activity of lipase. Strikingly, lipase activity in GNP_{528}-doped reverse micelles increases with an increase in W_0 value, a result contrary to CTAB reverse micelles without GNPs. It was also observed that a structurally deprived lipase induced by GNPs can also exhibit improved activity in reverse micelles, which further reiterates the activating effect of the reverse-micellar system. Therefore, this report is, to the best of our knowledge, the first that delineates the role of GNPs in enhancing the activity of lipase in reverse micelles. This study will pave the pathway for future work in which the unique properties of GNPs can be utilized to activate enzymes and biocatalytic processes.

Experimental Section

Materials: *Chromobacterium viscosum* lipase (E.C.3.1.1.3 type XII), trypsin (E.C.3.4.21.4, type I from bovine pancreas), $[HAuCl_4]$ (30 wt%) in solution with water, and *N*-α-benzyloxycarbonyl-L-lysine-*p*-nitrophenyl ester hydrochloride were purchased from Sigma (USA) and were used as received. Analytical-grade CTAB was purchased from Spectrochem (India) and was recrystallized three times from methanol/diethyl ether. Recrystallized CTAB was without minima in a surface-tension plot. IR-grade KBr, *n*-propyl bromide, *n*-hexadecylamine, HPLC-grade isooctane, *n*-hexanol, iodomethane, $NaBH_4$, and all the other reagents were purchased from Spectrochem and SRL (India) and were of the highest analytical grade. Trisodium citrate was procured from Merck (India). UV/Vis absorption spectra were recorded on a Varian Cary-50 spectrophotometer. A Bruker Advance DPX-300 spectrophotometer was used to perform the ^1H NMR spectroscopic analysis. CD spectroscopy was carried out on a Jasco J-815 spectrometer. FTIR spectra were recorded on a Perkin–Elmer Spectrum 100 FTIR spectrometer. Lyophilization was carried out in a Virtis 4KBTXL-75 freeze drier. Substrates for lipase *p*-nitrophenyl *n*-octanoate and *p*-nitrophenyl *n*-hexanoate and surfactant CTPAB were synthesized following previously reported protocols.[11a,13d,e]

Preparation of different GNP solutions

Synthesis of citrate-reduced and -capped GNP (GNP_{528}): $[HAuCl_4]$ in water (68 μL, 89 mM) was added to water (4.7 mL) in a 5-mL volumetric flask. The reaction mixture was stirred and heated to 70 °C. Freshly prepared aqueous trisodium citrate solution (250 μL, 169.4 mM) was added dropwise to this hot solution and the heating was continued for 15 min. A wine-red solution was formed that showed an SPR peak at 528 nm in the UV/Vis spectra.

Synthesis of borohydride-reduced and citrate-capped GNP

1) Synthesis of GNP_{511}: Ice-cold, freshly prepared aqueous $NaBH_4$ solution (150 μL, 0.1 M) was added to an aqueous solution (5 mL) of $[HAuCl_4]$ (0.3 mM) and trisodium citrate (0.3 mM) with stirring. The final concentration of the $NaBH_4$ solution was 3 mM, and the concentration ratio of $[Au]/[citrate]/[NaBH_4]$ was 1:1:10. The solution immediately turned pink after the addition of $NaBH_4$, thus indicating the formation GNPs. The SPR peak of the solution was at 511 nm.

2) Synthesis of GNP_{529}: A similar procedure to the preparation of GNP_{511} was followed, except that the volume of the aqueous $NaBH_4$ solution (0.1 M) used. Ice-cold, freshly prepared aqueous $NaBH_4$ solution (52.5 μL, 0.1 M) was used as the reducing agent. The final concentration of the $NaBH_4$ solution was 1.05 mM, and the concentration ratio of $[Au]/[citrate]/[NaBH_4]$ was 1:1:3.5.The solution turned wine red, and the SPR peak of the solution was at 529 nm.

3) Synthesis of GNP_{536}: The same method was followed. Ice-cold, freshly prepared aqueous $NaBH_4$ solution (30 μL, 0.1 M) was used the reducing agent. The final concentration of the $NaBH_4$ solution was 0.6 mM, and the concentration ratio of $[Au]/[citrate]/[NaBH_4]$ was 1:1:2. The solution turned wine red, and the SPR peak of that solution was at 536 nm.

Synthesis of borohydride-reduced GNP: Ice-cold, freshly prepared aqueous $NaBH_4$ solution (150 μL, 0.1 M) was added to an aqueous solution of $[HAuCl_4]$ (5 mL, 0.3 mM) with stirring. The final concentration of the $NaBH_4$ solution was 3 mM. The solution immediately turned pink after the addition of $NaBH_4$, thus indicating the formation GNPs. The SPR peak of the solution was at 512 nm.

Preparation of reverse micelles with GNPs synthesized in situ: An aqueous solution containing $[HAuCl_4]$ (30 mM) and trisodium citrate (60 mM) was used to make a CTAB (50 mM)/iso-octane/*n*-hexanol/water microemulsion system at the required z and W_0 values. A similar CTAB reverse micelle was formed with an aqueous solution of $NaBH_4$ (0.1 M) at comparable z and W_0 values. This microemulsion was added dropwise to the reverse micelle containing $[HAuCl_4]$ with stirring. The reaction mixture was vortexed for a about 2 min to obtain perfect mixing. The color of the resultant reverse micelle quickly turned red–pink. The final concentration ratio of $[Au]/[citrate]/[NaBH_4]$ was 1:1:10 in which the Au concentration varied from 10 to 12 μM. The SPR peak was of the solution was at 514 nm.

The reverse micelles with GNPs synthesized in situ were also formed by reduction with only $NaBH_4$ without using trisodium citrate as the capping agent by following the above protocol.

Preparation of reverse micelles and GNP-doped reverse micelles: The requisite quantity of surfactant was dispersed in iso-octane in a 2-mL volumetric flask to which a calculated amount of *n*-hexanol was added to attain the corresponding *z* value and shaken vigorously. Finally, aqueous buffer (phosphate) solution was added (to reach the corresponding W_0 value), and the whole suspension was vortexed to obtain a clear homogeneous solution of CTAB or CTPAB (50 mM)/iso-octane/*n*-hexanol/water reverse micelle. A similar protocol was followed to obtain the GNP-doped reverse micelle. A solution of GNP in water was added instead of buffer. During the preparation of the reverse micelle with a lower concentration of the GNPs, phosphate buffer solution was added so that the GNP solution obtained the corresponding W_0 value and the desired GNP concentration.

Activity of interfacially solubilized lipase in reverse micelles: The second-order rate constant k_2 in the lipase-catalyzed hydrolysis of *p*-nitrophenyl *n*-octanoate in cationic w/o microemulsions was determined spectrophotometrically at the isosbestic points (see Table S1 in the Supporting Information) as reported previously.[11a,13d,15,16] In a typical experiment, the aqueous enzyme stock solution (4.5 μL, 0.34 mg mL^{-1}) and substrate stock solution in iso-octane (10 μL, 0.45 M) were added to the w/o microemulsion (1.5 mL) previously prepared at the desired surfactant concentration and pH value (i.e., the pH value of the aqueous buffer solutions used for preparing the w/o microemulsions; the pH value within the water pool of the w/o microemulsions did not vary significantly: <1 unit)[16,23] in a cuvette to attain the particular W_0 value and reactant concentrations. Gentle shaking produced clarification of the microemulsion within 1 min. The initial linear rate of increase in the absorbance of liberated *p*-nitrophenol was recorded at the isosbestic points λ_{iso}. The molar extinction coefficients ε at isosbestic point and the λ_{iso} value of the *p*-nitrophenol/*p*-nitrophenolate couple in w/o microemulsions of different systems with varying GNP concentrations are given in Table S1 in the Supporting Information. The overall concentrations of lipase and *p*-nitrophenyl *n*-octanoate were 1.02×10^{-6} g mL^{-1} and 3×10^{-3} M, respectively. Although the lipase was essentially confined to the dispersed water droplets (at the oil/water interface), for simplicity, the concentration of reactants were referred to the overall concentration to avoid the complexity of the volume fraction of the water droplet in the w/o microemulsions and the partitioning coefficient of the substrate.[13d,23] Moreover, we measured the second-order rate constant k_2 instead of the first-order Michaelis–Menten catalytic constant k_{cat} because the initial rate of the lipase-catalyzed hydrolysis of *p*-nitrophenyl alkanoate was first order with respect to the substrate concentration (see Figure S2 in the Supporting Information).[13d,15,16,23] The pH aqueous solutions of GNP_{511}, GNP_{528}, GNP_{529}, and GNP_{536} were 8.0, 5.6, 5.3, and 5.0, respectively. In the absence of GNPs, the lipase activities in the control experiments were measured at the respective pH values and all the other experimental conditions were kept identical. It is already known that lipase activity remains almost same within the range pH 2–10 in CTAB reverse micelles.[14a] We also observed that by varying the pH value, the lipase activity remains same as observed for pH 6 (20 mM phosphate buffer).

Activity of lipase in water + 4% EtOH: The second-order rate constant k_2 of the lipase-catalyzed hydrolysis of *p*-nitrophenyl *n*-hexanoate in water was determined spectrophotometrically at the isosbestic points. CV lipase also obeys second-order kinetics in water + 4% EtOH.[16] For total solubilization of the substrate, we used substrate and enzyme concentrations that were 50-fold lower than that for w/o microemulsions. Thus, the final concentration of the substrate was 0.06 mM and lipase was 0.02×10^{-6} g cm^{-3}. The isosbestic point and molar extinction coefficient at λ_{iso} (340 nm) of the *p*-nitrophenol/*p*-nitrophenolate couple in water + 4% EtOH without GNPs and with GNPs were 6500 and 6250 M^{-1} cm^{-1}, respectively.

Activity measurement of trypsin

1) Substrate solution: A stock solution of the substrate *N*-α-benzyloxycarbonyl-L-lysine-*p*-nitrophenyl ester hydrochloride (20–250 mM) was prepared in HPLC-grade dimethyl sulfoxide (DMSO). An aliquot of the stock solution (6 μL) was added to the reverse micelle solution (1.5 mL) in the cuvette, which was shaken to achieve a reaction concentration of the substrate of 20–250 μM.

2) Enzyme solution: Trypsin stock solution (1.2×10^{-3} M) was prepared in buffer solution (1 mL, pH 3; containing $CaCl_2$ (1 mM)) and diluted tenfold with phosphate buffer solution (pH 6, 20 mM) just before use. The diluted solution (4 μL) was added to the reverse micelle solution (1.5 mL) to reach an overall trypsin concentration of 0.32 μM in the cuvette.

3) Enzyme kinetics: The kinetic parameters k_{cat} of the compartmentalized trypsin-catalyzed hydrolysis (trypsin: 0.32 μM) of *N*-α-benzyloxycarbonyl-L-lysine-*p*-nitrophenyl ester hydrochloride in CTAB reverse micelles were determined spectrophotometrically[11e] by following the formation of *p*-nitrophenol at the isosbestic points. The isosbestic point and molar extinction coefficient at λ_{iso} of the *p*-nitrophenol/*p*-nitrophenolate couple in CTAB (50 mM)/water/iso-octane/*n*-hexanol and in GNP-doped CTAB reverse micelles are shown in Table S1. In a typical experiment, aliquots of the different substrate stock solutions (6 μL, 20–250 mM in HPLC-grade DMSO) were added to the reverse micelles (1.5 mL; previously prepared at the desired surfactant concentration and pH value in a cuvette). The activity of the enzyme was monitored spectrophotometrically at the isosbestic point by adding the diluted enzyme solution (4 μL) to the cuvette. The trypsin activity was studied at pH 6 rather than at the optimum pH value (around 8.0) primarily to prevent spontaneous chemical hydrolysis of the substrate in the cationic reverse micelles and to facilitate the operational stability of the enzyme because the formation of *p*-nitrophenol is most convenient to follow at steady state. The overall reaction concentration of trypsin was 0.32 μM. The initial velocities were plotted against the concentration of the substrate and the experimental data were fitted to a linearized Michaelis–Menten plot to determine the k_{cat} values (s^{-1}).

CD spectra: The CD spectra of lipase and GNP/lipase in reverse micelles were recorded on Jasco J-815 spectrometer in a 2-mm path-length cell at $\lambda=220$–300 nm with a scan speed of 50 nm min^{-1} (in the case of reverse micelles, the CD spectra could not be measured below $\lambda=220$ nm due to an off-scale signal). For GNP/lipase in water, the spectra were recorded in a 10-mm path-length cell at $\lambda=200$–300 nm. All the spectra were corrected by subtracting a blank spectrum (without enzyme) and accumulated six times. The results are expressed in terms of mean residue ellipticity (deg cm^2 dmol^{-1}). The final concentration of the lipase was kept at 25 μg mL^{-1} in the reverse micelle and 10 μg mL^{-1} in water.

FTIR spectroscopy: For the FTIR spectra of GNP/lipase, lipase solution (500 μL, 0.34 mg mL^{-1}) in water was mixed with GNP_{528} in water (560 μL, 1.2 mM) and lyophilized for 24 h. For native lipase, the lipase solution (500 μL, 0.34 mg mL^{-1}) was lyophilized. These lyophilized powders were carefully transferred into a mortar containing IR-grade KBr (ca. 30 mg) and were ground to prepare the pellet under strictly dry conditions to prevent absorption of water vapor. This pellet was further dried by storing in a vacuum desiccator. Spectra of the pellets were recorded and accumulated 512 times at a resolution of 2 cm^{-1} with intervals of 1 cm^{-1}. The FTIR spectrum with lyophilized Au (from identical compositions without lipase) was also recorded and subtracted from the spectrum of the GNP/lipase mixture to obtain the spectra of just the protein.

Quantification of secondary structure of lipase and GNP/lipase: The amide I region from $\tilde{\nu}=1600$ to 1700 cm^{-1} was analyzed to quantify the secondary structural contents of the enzymes. The different spectra were smoothed by a nine-point Savitsky–Golay smoothing function with the help of software supplied with the Perkin–Elmer FTIR spectrometer. A straight baseline was obtained in the region from $\tilde{\nu}=1750$ to 2000 cm^{-1}, an important prerequisite in obtaining quantitative structural information. Fourier deconvolution was performed using the Perkin–Elmer software with a line-narrowing factor $k=2.3$ and half bandwidth of 37 cm^{-1}. The second-derivative spectrum was obtained from the deconvoluted spectra with Savitsky–Golay derivative function software with a five-point window. α-Helical and β-sheet structures were assigned by following the previous reports.[19] The relative amounts of the α helices and β sheets were determined by computing the areas under the assigned bands. Each sample was measured four times.

TEM studies: Aliquots of the GNP solutions (4 μL; either in water or reverse micelles) were placed on a 300-mesh Cu-coated TEM grid and dried under vacuum for 4 h before taking the TEM images. The TEM measurements were performed on a JEOL JEM 2010 microscope.

DLS studies: The DLS measurements were performed with a fixed-angle apparatus (Brookhaven Instruments Corporation, USA) equipped with a Melles Griot HeNe laser (Model BI-200SM Goniometer VER-2.0 plus particle-size analyzer operating at $\lambda = 633$ nm) with 35 mW of power. The sample solutions were filtered through 0.22-μm Millipore filters three or four times before each experiment. The scattering intensity data collected under different conditions were computed by a data processor with necessary software.[24]

Acknowledgements

P.K.D. is thankful to the Department of Science and Technology (Government of India) for financial assistance through the Ramanna Fellowship (no. SR/S1/RFPC-04/2006). S.M., D.D, and A.S acknowledge the CSIR (India) for their Research Fellowships.

[1] I. Sosa, C. Noguez, R. Barrera, *J. Phys. Chem. B* **2003**, *107*, 6269.
[2] A. N. Shipway, M. Lahav, I. Willner, *Adv. Mater.* **2000**, *12*, 993.
[3] K. Chi-Lap, C. Wei-Yu, C. Yu-Chie, *Anal. Bioanal. Chem.* **2007**, *387*, 2091.
[4] a) I. Willner, R. Baron, B. Willner, *Adv. Mater.* **2006**, *18*, 1109; b) C. A. Mirkin, R. L. Letsinger, R. C. Mucic, J. J. Storhoff, *Nature* **1996**, *382*, 607; c) Z. Li, S. W. Chung, J. M. Nam, D. S. Ginger, C. A. Mirkin, *Angew. Chem.* **2003**, *115*, 2408; *Angew. Chem. Int. Ed.* **2003**, *42*, 2306.
[5] a) M. Brust, M. Walker, D. Bethell, D. J. Schiffrin, R. Whyman, *J. Chem. Soc. Chem. Commun.* **1994**, 801; b) J. Turkevich, P. C. Stevenson, J. Hillier, *Discuss. Faraday Soc.* **1951**, *11*, 55; c) G. Frens, *Nat. Phys. Sci.* **1973**, *20*, 241; d) N. R. Jana, L. Gearheart, C. J. Murphy, *J. Phys. Chem. B* **2001**, *105*, 4065; e) J. Kimling, M. Maier, B. Okenve, V. Kotaidis, H. Ballot, A. Plech, *J. Phys. Chem. B* **2006**, *110*, 15700; f) A. P. Herrera, O. Resto, J. G. Briano, C. Rinaldi, *Nanotechnology* **2005**, *16*, s618, and reference therein; g) C. Feng, L. Gu, D. Yang, J. Hu, G. Lu, X. Huang, *Polymer* **2009**, *50*, 3990; h) B. Pan, D. Cui, P. Xu, Q. Li, T. Huang, R. He, F. Gao, *Colloids Surf. A* **2007**, *295*, 217; i) J. Lin, W. Zhou, C. J. O'Connor, *Mater. Lett.* **2001**, *49*, 282.
[6] a) R. Jin, Y. C. Cao, C. A. Mirkin, K. L. Kelly, G. C. Schatz, *Science* **2001**, *294*, 1901; b) F. Kim, S. Connor, H. Song, T. Kuykendall, P. Yang, *Angew. Chem.* **2004**, *116*, 3699; *Angew. Chem. Int. Ed.* **2004**, *43*, 3615; c) M. Sakamoto, T. Tachikawa, M. Fujitsuka, T. Majima, *Adv. Funct. Mater.* **2007**, *17*, 857; d) R. N. Mitra, P. K. Das, *J. Phys. Chem. C* **2008**, *112*, 8159.
[7] a) C. Avelino, G. Hermenegildo, M. N. Pedro, P. Ana, C. J. Jose, T. Susana, *Chem. Eur. J.* **2007**, *13*, 6359; b) H. Hua, X. Chao, R. Jicun, *Anal. Chem.* **2008**, *80*, 5951.
[8] a) C.-C You, S. S. Agasti, M. De, M. J. Knapp, V. M. Rotello, *J. Am. Chem. Soc.* **2006**, *128*, 14612; b) A. Verma, J. M. Simard, J. W. E. Worrall, V. M. Rotello, *J. Am. Chem. Soc.* **2004**, *126*, 13987; c) C. C. You, A. Verma, V. M. Rotello, *Soft Matter* **2006**, *2*, 190.
[9] a) Y. F. Huang, C. C. Huang, H. T. Chang, *Langmuir* **2003**, *19*, 7498; b) C-C. You, R. R. Arvizo, V. M. Rotello, *Chem. Commun.* **2006**, 2905; c) A. Verma , V. M. Rotello, *Chem. Commun.* **2005**, 303.
[10] a) P. L. Luisi, L. J. Magid, *CRC Crit. Rev. Bioeng.* **1986**, *20*, 409; b) K. Martinek, A. V. Levashov, Y. L. Khmelnitsky, N. L. Klyachko, I. V. Berezin, *Science* **1982**, *218*, 889; c) M. A. Biasutti, E. B. Abuin, J. J. Silber, N. M. Correa, E. A. Lissi, *Adv. Colloid Interface Sci.* **2008**, *136*, 1; d) F. M. Menger, *Angew. Chem.* **1991**, *103*, 1104; *Angew. Chem. Int. Ed. Engl.* **1991**, *30*, 1086; e) K. Martinek, A. V. Levashov, N. L. Klyachko, A. V. Kabanov, Y. L. Khmelnitsky, *Biochim. Biophys. Acta* **1989**, *981*, 161; f) V. Brissos, E. P. Melo, J. M. G. Martinho, J. M. S. Cabral, *Biochim. Biophys. Acta* **2008**, *1784*, 1326; g) P. Walde, D. Han, P. L. Luisi, *Biochemistry* **1993**, *32*, 4029; h) F. X. Yang, A. J. Russell, *Biotechnol. Bioeng.* **1995**, *47*, 60; i) R. Biswas, A. R. Das, T. Pradhan, D. Touraud, W. Kunz, S. Mahiuddin, *J. Phys. Chem. B* **2008**, *112*, 6620.
[11] a) A. Shome, S. Roy, P. K. Das, *Langmuir* **2007**, *23*, 4130; b) A. Dasgupta, D. Das, R. N. Mitra, P. K. Das, *J. Colloid Interface Sci.* **2005**, *289*, 566; c) T. Maruyama, T. Hosogi, M. Goto, *Chem. Commun.* **2007**, 4450; d) C. Oldfield, R. B. Freedman, B. H. Robinson, *Faraday Discuss.* **2005**, *129*, 247; e) A. Dasgupta, D. Das, P. K. Das, *Biochimie* **2005**, *87*, 1111.
[12] a) A. S. Bommarius, T. A. Hatton, D. I. C. Wang, *J. Am. Chem. Soc.* **1995**, *117*, 4515; b) E. Lissi, E. Abuin, *Langmuir* **2000**, *16*, 10084; c) E. Abuin, E. Lissi, R. Duarte, *Langmuir* **2003**, *19*, 5374; d) S. Mahiuddin, A. Renoncourt, P. Bauduin, D. Touraud, W. Kunz, *Langmuir* **2005**, *21*, 5259; e) R. D. Falcone, M. A. Biasutti, N. M. Correa, J. J. Silber, E. Lissi, E. Abuin, *Langmuir* **2004**, *20*, 5732; f) P. Bauduin, D. Touraud, W. Kunz, M. P. Savelli, S. Pulvin, B. W. J. Ninham, *J. Colloid Interface Sci.* **2005**, *292*, 244.
[13] a) C. M. L. Carvalho, M. R. Aires-Barros, J. M. S. Cabral, *Langmuir* **2000**, *16*, 3082; b) C. M. L. Carvalho, J. M. S. Cabral, *Biochimie* **2000**, *82*, 1063; c) A. M. Azevedo, L. P. Fonseca, D. Graham, J. M. S. Cabral, D. M. F. Prazeres, *Biocatal. Biotransform.* **2001**, *19*, 213; d) D. Das, P. K. Das, *Langmuir* **2003**, *19*, 9114; e) D. Das, S. Roy, R. N. Mitra, A. Dasgupta, P. K. Das, *Chem. Eur. J.* **2005**, *11*, 4881; f) M. C. Pinna, P. Bauduin, D. Touraud, M. Monduzzi, B. W. Ninham, W. Kunz, *J. Phys. Chem. B* **2005**, *109*, 16511.
[14] a) R. N. Mitra, A. Dasgupta, D. Das, S. Roy, S. Debnath, P. K. Das, *Langmuir* **2005**, *21*, 12115; b) S. Roy, A. Dasgupta, P. K. Das, *Langmuir* **2006**, *22*, 4567; c) C. Schirmer, Y. Liu, D. Touraud, A. Meziani, S. Pulvin, W. Kunz, *J. Phys. Chem. B* **2002**, *106*, 7414; d) S. Debnath, A. Dasgupta, R. N. Mitra, P. K. Das, *Langmuir* **2006**, *22*, 8732; e) D. Das, P. K. Das, *Langmuir* **2009**, *25*, 4421; f) B. Minofar, R. Vacha, A. Wahab, S. Mahiuddin, W. Kunz, P. Jungwirth, *J. Phys. Chem. B* **2006**, *110*, 15939; g) E. P. Melo, R. P. Baptista, J. M. S. Cabral, *J. Mol. Catal. B* **2003**, *22*, 299.
[15] P. K. Das, A. Chaudhuri, *Langmuir* **2000**, *16*, 76.
[16] P. D. I. Fletcher, B. H. Robinson, R. B. Freedman, C. Oldfield, *J. Chem. Soc. Faraday Trans.* **1985**, *81*, 2667.
[17] a) T. R. J. Jenta, T. Batts, G. D. Rees, B. H. Robinson, *Biotechnol. Bioeng.* **1997**, *54*, 416; b) G. W. Zhou, G. Z. Li, J. Xu, Q. Sheng, *Colloids Surf. A* **2001**, *176–195*, 194.
[18] a) D. Das, D. Das, P. K. Das, *Biochimie* **2008**, *90*, 820; b) S. Debnath, D. Das, P. K. Das, *Biochem. Biophys. Res. Commun.* **2007**, *356*, 163.
[19] a) A. Dong, P. Huang, W. S. Caughey, *Biochemistry* **1990**, *29*, 3303; b) W. Al-Azzam, E. A. Pastrana, Y. Ferrer, Q. Huang, R. Schweitzer-Stenner, K. Griebenow, *Biophys. J.* **2002**, *83*, 3637; c) K. Griebenow, A. M. Klibanov, *J. Am. Chem. Soc.* **1996**, *118*, 11695.
[20] a) A. Gole, C. Dash, C. Soman, S. R. Sainkar, M. Rao, M. Sastry, *Bioconjugate Chem.* **2001**, *12*, 684; b) A. L. Crumbliss, S. C. Perine, J. Stonehuerner, K. R. Tubergen, Junguo Zhao, R. W. Henkens, J. P. O'Daly, *Biotechnol. Bioeng.* **1992**, *40*, 483.
[21] a) S. S. Atik, J. K. Thomas, *J. Am. Chem. Soc.* **1981**, *103*, 4367; b) E. M. Corbeil, N. E. Levinger, *Langmuir* **2003**, *19*, 7264.
[22] P. K. Das, A. Chaudhuri, S. Saha, A. Samanta, *Langmuir* **1999**, *15*, 4765.
[23] P. K. Das, A. Chaudhuri, *Langmuir* **1999**, *15*, 8771.
[24] The second-order rate kinetics, isosbestic points and corresponding molar extinction coefficients, lipase activities in CTPAB reverse micelles, and the TEM images of GNPs entrapped in reverse micelles are provided in the Supporting Information.

Received: May 15, 2009
Revised: October 16, 2009
Published online: December 10, 2009

